Front. Optoelectron. 2013, 6(2): 167–174
DOI 10.1007/s12200-013-0306-1

RESEARCH ARTICLE

High precision mode of subaperture stitching for optical surfaces measurement

Huijing ZHANG[1], Haobo CHENG (✉)[1], Hon Yuen TAM[2], Yongfu WEN[1], Dongmei ZHOU[1]

1 School of Optoelectronics, Beijing Institute of Technology, Beijing 100081, China
2 Department of Mechanical and Biomedical Engineering, City University of Hong Kong, Hong Kong, China

© Higher Education Press and Springer-Verlag Berlin Heidelberg 2013

Abstract Subaperture stitching (SAS) provides us with an attractive way of extending the effective aperture and dynamic range of phase measuring interferometers. Accuracy of stitching algorithm becomes the key factor in the SAS technology. In this paper, the basic principle of SAS was introduced and four modes of SAS were discussed. The stitching experiments were done through the SSI-300 workstation designed and developed independently. There were several comparisons between the four different stitching methods and the measurement of full aperture. The results suggest that the global error averaging mode with reference of subaperture near optic axis is of high precision.

Keywords optical testing, subaperture stitching (SAS), algorithm, stitching mode

1 Introduction

Rapid development of science and technology calls for higher requirements for the aspheric manufacture, such as larger aperture and ultra precision [1–4]. High-precision aspheric surface manufacture depends on relevant high-precision testing method and equipment, which is important for testing larger aperture and high-precision aspheric surface. Compared with other measurement methods, such as structure-light measuring technique and phase-measuring profilometry, interferometry has the advantages in high resolution, high sensitivity, high reproducibility, etc [5–7]. Therefore, this technique has become a primary method in optical surface shape testing. For aspheric testing, common null test requires special compensator for each aspheric. And it is difficult to design, fabricate, test and adjust the compensator and is of high cost [8]. In addition, for the test of the large-aperture plane, the high cost of the large-aperture interferometer prohibits itself wider application in testing large aperture optics.

Subaperture stitching (SAS) without other auxiliary components provides us with an attractive way of extending the effective aperture and dynamic range of phase measuring interferometers. This method could not only improve the resolution and save costs, but also shorten the construction period. The SAS method to test large-aperture mirror was carried out in the 1980s overseas [9–11] and now it is in the development stage of applied research and commercial instruments. But this technology in China, which has made some progress since 1990s, is still at the experimental stage [12,13].

In this paper, method for improving precision of SAS that using a high precision mode is proposed. In Section2, the basic principle of the SAS is given. In Section 3, the stitching modes which affect precision are discussed, and according to error averaging, the global error averaging mode near optic axis is given. In Section 4, four different stitching modes are compared by experiments, and then the optimal algorithm of data stitching mode is obtained. Finally, the conclusion is presented in Section 5.

2 Principle of SAS interferometer

The way of SAS interferometry is to measure the glass part by part with a small-aperture interferometer, the measurements results are connected together with minimizing the error of the phase distributions in common area [14].

Taking the connection of two circular subapertures as an example shown in Fig. 1, Φ_1 and Φ_2 are the testing results of the two subapertures.

$\Phi_1(x,y)$ and $\Phi_2(x,y)$ respectively indicate the phase distributions of the two tested subapertures as follows:

Received December 5, 2012; accepted March 4, 2013

E-mail: chenghaobo@tsinghua.org.cn

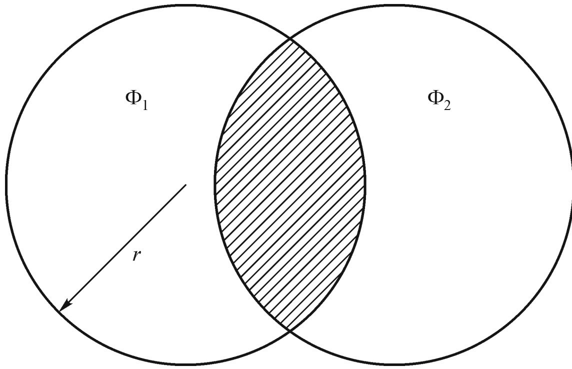

Fig. 1 Two circular stitching schematic diagram

$$\begin{cases} \Phi_1(x,y) = P_1 + T_{x1}x + T_{y1}y + \Phi_0(x,y), \\ \Phi_2(x,y) = P_2 + T_{x2}x + T_{y2}y + \Phi_0(x,y), \end{cases} \tag{1}$$

where $\Phi_0(x,y)$ is the system coordinate, P_i is the offset along optical axis, T_{xi} and T_{yj} respectively present the gradient along x-axis and y-axis. The overlap section of Φ_1 and Φ_2 has the same phase, which is used to measure the testing difference and determine the relative gradient and axial displacement. The above equation is simplified as

$$\Delta\Phi = \Delta P + \Delta T_x x + \Delta T_y y, \tag{2}$$

where $\Delta P = p_1 - p_2$, $\Delta T_x = T_{x1} - T_{x2}$, $\Delta T_y = T_{y1} - T_{y2}$.

Theoretically, the exact solutions of ΔP, ΔT_x, ΔT_y can be obtained only by three points, which is not in a line in the overlap region. However, considering the influence of error, more points should be calculated to obtain the three parameters with the least square fitting to reduce the error effect.

In the stitching process, the wavefront of full aperture can be retrieved in the premise that the full aperture is totally overcovered through several subaperture stitching, and at the same time, the adjacent subapertures should hold a certain overlap section.

3 Stitching mode

In the course of actual measurement, stitching mode selection refers to the selection of order and path of subaperture stitching. There are four common stitching modes, such as serial mode, parallel mode, global error averaging mode and partial error averaging mode [15–17].

Serial mode means that the latter subaperture is stitched to the former one in sequence. This case would lead to an accumulation of errors because every stitching has error. Parallel mode is to select a subaperture as a reference and stitch all other subapertures together with it. Partial error averaging mode is that the subaperture fitted and stitched is the basis of latter stitching and then used to be fitted and stitched with the latter subaperture, which is the improved algorithm of serial stitching [16]. Global error averaging mode is to use an arbitrary subaperture as reference, and calculate the stitching factor of other subapertures relative to the reference in the premise of minimizing the residual sum of squares of all overlapping areas [18].

In this paper, we select the subaperture near the optical axis as reference, which is called the global error averaging mode with reference of subaperture near optic axis. Assuming that there are M subapertures to stitch, called $A_1,A_2,\ldots,A_M$. The subaperture data were obtained in sequence. A_m is reference aperture, and the transformation coefficients of other aperture relative to A_m are (a_1,b_1,c_1), $(a_2,b_2,c_2),\ldots,(a_M,b_M,c_M)$. So these transformation coefficients satisfy the following equation.

$$\begin{aligned} \Phi_m(x,y) &= \Phi_0(x-x_0,y-y_0) + a_0x + b_0y + c_0 \\ &= \Phi_1(x-x_1,y-y_1) + a_1x + b_1y + c_1 \\ &\vdots \\ &= \Phi_{m-1}(x-x_{m-1},y-y_{m-1}) + a_{m-1}x \\ &\quad + b_{m-1}y + c_{m-1} \\ &= \Phi_{m+1}(x-x_{m+1},y-y_{m+1}) + a_{m+1}x \\ &\quad + b_{m+1}y + c_{m+1} \\ &\vdots \\ &= \Phi_{M-1}(x-x_{M-1},y-y_{M-1}) + a_{M-1}x \\ &\quad + b_{M-1}y + c_{M-1}, \end{aligned} \tag{3}$$

where $\Phi_0,\Phi_1,\ldots,\Phi_{M-1}$ are the phase distributions of A_1, $A_2,\ldots,A_M$ respectively. The least-squares is used to minimize the sum of squared difference in the common areas as

$$\begin{aligned} &\sum_0 \{\Phi(x,y) - [\Phi_0(x-x_0,y-y_0) + a_0x + b_0y + c_0]\}^2 \\ &+ \sum_1 \{\Phi(x,y) - [\Phi_1(x-x_1,y-y_1) + a_1x + b_1y + c_1]\}^2 \\ &+ \cdots \\ &+ \sum_{m-1} \{\Phi(x,y) - [\Phi_{m-1}(x-x_{m-1},y-y_{m-1}) \\ &+ a_{m-1}x + b_{m-1}y + c_{m-1}]\}^2 \\ &+ \sum_{m+1} \{\Phi(x,y) - [\Phi_{m+1}(x-x_{m+1},y-y_{m+1}) \\ &+ a_{m+1}x + b_{m+1}y + c_{m+1}]\}^2 + \cdots \\ &+ \sum_{M-1} \{\Phi(x,y) - [\Phi_{M-1}(x-x_{M-1},y-y_{M-1}) \\ &+ a_{M-1}x + b_{M-1}y + c_{M-1}]\}^2 \\ &\rightarrow \min, \end{aligned} \tag{4}$$

where summations are taken in the common areas with any

overlapping measurements. The unknown number is $3\times(M-1)$ since a_m, b_m, c_m are not included.

The partial derivative of Eq. (4) with respect to each unknown is calculated, and the least-squares equation can be obtained

$$\left[\left(\sum_{k}^{M-1}P_{ik}\right)\right]\left[\left(Q_{ij}-\delta_{ij}\sum_{k}^{M-1}Q_{ik}\right)_{ij}\right][(R_i)_i]=0, \quad (5)$$

where the expressions in parenthesis represent the elements of the matrix, both i and j are the integer from 0 to $M-1$ (m is not included), k is the integer from 0 to $M-1$ (m is included), and δ_{ij} is Kronecker delta function as follow

$$\delta_{ij}=\begin{cases}1, & i=j,\\ 0, & i\neq j,\end{cases} \quad (6)$$

$$P_{ij}=\begin{bmatrix}\sum\limits_{i\cap j}x\Delta(x,y)\\ \sum\limits_{i\cap j}y\Delta(x,y)\\ \sum\limits_{i\cap j}\Delta(x,y)\end{bmatrix}, \quad (7)$$

$$Q_{ij}=\begin{bmatrix}\sum\limits_{i\cap j}x^2 & \sum\limits_{i\cap j}xy & \sum\limits_{i\cap j}x\\ \sum\limits_{i\cap j}xy & \sum\limits_{i\cap j}y^2 & \sum\limits_{i\cap j}y\\ \sum\limits_{i\cap j}x & \sum\limits_{i\cap j}y & n_{ij}\end{bmatrix}, \quad (8)$$

$$R_i=\begin{bmatrix}a_i\\ b_i\\ c_i\end{bmatrix}, \quad (9)$$

where n_{ij} is the number of sampling points in overlapping area, and all x and y coordinates are taken in the global coordinate system based on area A_m. The addition in Eqs. (7) and (8) would work only in overlapping area. If there is no overlapping between the two adjacent subapertures, P_{ij} and Q_{ij} become null matrices.

Transform coefficients R_i can be got by solving Eq. (5). These data can be used to align individual measurements to obtain the entire shape of the sample.

Every configuration parameters can be obtained by solving Eq. (5), and then be used to compensate configuration parameter of subaperture.

4 Stitching experiment

Independent R&D subaperture stitching interferometry (SSI-300) workstation with six-dimension was used for the experiments. The structure of SSI-300 is shown in Fig. 2.

The Twyman Green interferometer used in the workstation is fixed on z-axis vertically. The tested surface is fixed on the five axis stages including horizontal movement along x and y direction, tilt movement along x and y direction and 360° rotation around z direction. All these equipments are set up on an optical platform. A glass-ceramics plane standard mirror of diameter 130 mm was tested using 50 mm plane lens. To evaluate the precision of experimental result, we use indexes such as PV, RMS, ΔPV, ΔRMS and single point RMS. PV (peak-to-valley) gives a measure of the difference between the highest point and the lowest point of phase distribution in wavefront, it can be expressed as belows:

$$PV=\max_{1\leqslant i,j\leqslant N}\{W(i,j)\}-\min_{1\leqslant i,j\leqslant N}\{W(i,j)\}, \quad (10)$$

where ΔPV is the difference of PV between stitching result and measurement result. RMS stands for "root of the mean squares" and it is calculated as the standard deviation of the height (depth) of the test surface relative to the reference at all the data points in the wavefront [19]. It is expressed as the following equation:

$$RMS=\left[\frac{1}{N^2}\sum_{i,j=1}^{N^2}(W(i,j)-\langle W\rangle)^2\right]^{\frac{1}{2}}, \quad (11)$$

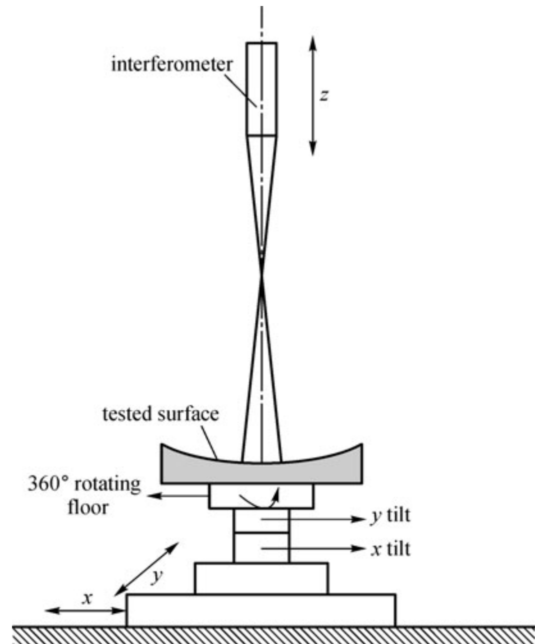

Fig. 2 SSI-300 structure

where $\langle W\rangle$ is the average value of phase distribution, it can be expressed as follows:

$$\langle W\rangle = \frac{1}{N^2}\sum_{i,j=1}^{N^2} W(i,j), \tag{12}$$

where N is the number of data points. ΔRMS represents the difference of RMS between stitching result and measurement result. Single-point RMS means the RMS of a single point in overlapping areas. It is calculated as

$$\delta_x = \frac{\sqrt{\sum_{i=1}^{n}(x_i - \overline{x})^2}}{n}, \tag{13}$$

where n is the number of subapertures, x_i is the measured value of ith subaperture, $\overline{x}$ is the mean arithmetical value of all the overlapping subapertures. The single-point RMS of the overlapping area can be got by calculating δ_x of every point in the whole overlapping area [20].

4.1 Stitching of five subapertures

The number and locations of subapertures are shown in Fig. 3.

Figure 4 shows the stitching results of five subapertures and the distribution of single point RMS in different stitching modes.

The stitching precision of five subapertures is given in Table 1.

4.2 Stitching of nine subapertures

The divided method of nine subapertures is shown in Fig. 5.

Figure 6 shows the stitching results of nine subaperture and the distribution of single point RMS in different stitching modes.

The stitching precision of nine subapertures is given in Table 2.

As shown in Figs. 4 and 6, the stitching surface figures of parallel mode, partial error averaging mode and global error averaging mode are all continuous and smooth. They can effectively reflect the full aperture surface shape after eliminating the tilt. But surface figure of serial stitching is not continuous, which is worse than those of another mode.

According to the single point RMS figures, along with the fitting and stitching in certain sequence, the stitching error of the serial mode is more obvious than that of another mode. It indicates that the serial mode would produce more serious error accumulation than that of another three modes, as the number of fitting stitching is less.

The precisions of subaperture stitching listed in Tables 1 and 2 show that serial mode has the worst precision in all

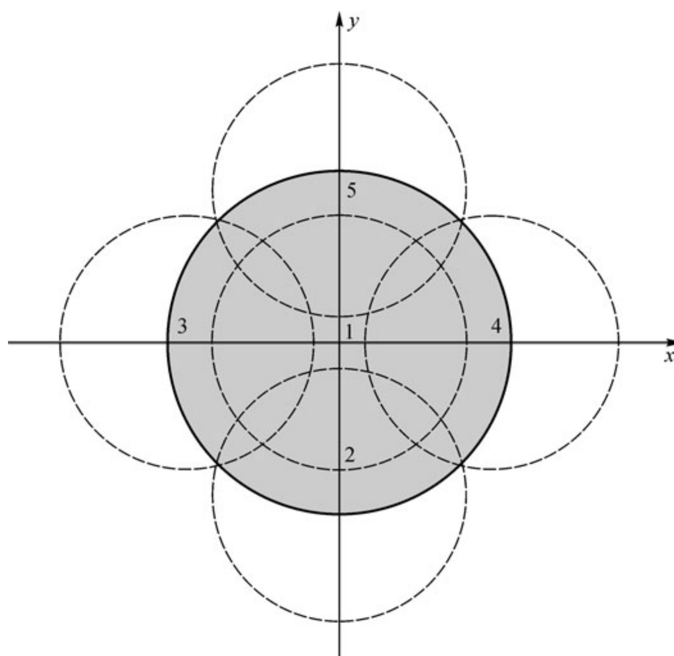

Fig. 3 Location of five subapertures

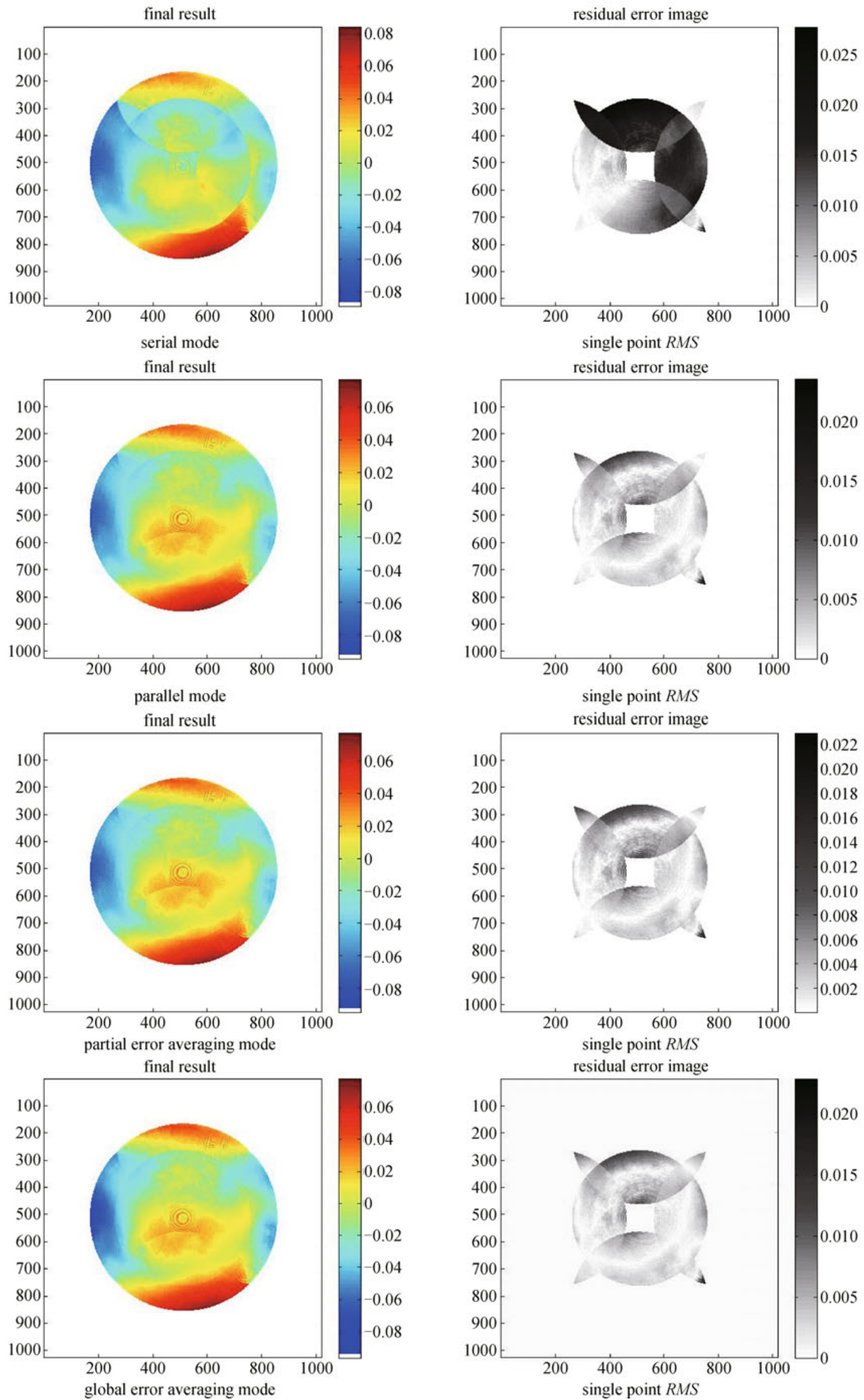

Fig. 4 Stitching results of five subapertures and single point *RMS* figures in different stitching modes

Table 1 Stitching precision of five subapertures ($\lambda = 632.8$ nm)

mode	*PV*	*RMS*	Δ*PV*	Δ*RMS*	single point *RMS*
serial mode	0.619400	0.146659	0.043231	0.000770	0.007130
parallel mode	0.619810	0.146303	0.043640	0.000414	0.002425
partial error averaging mode	0.621820	0.145947	0.045650	0.000059	0.002428
global error averaging mode	0.628718	0.145685	0.052549	0.000204	0.002507

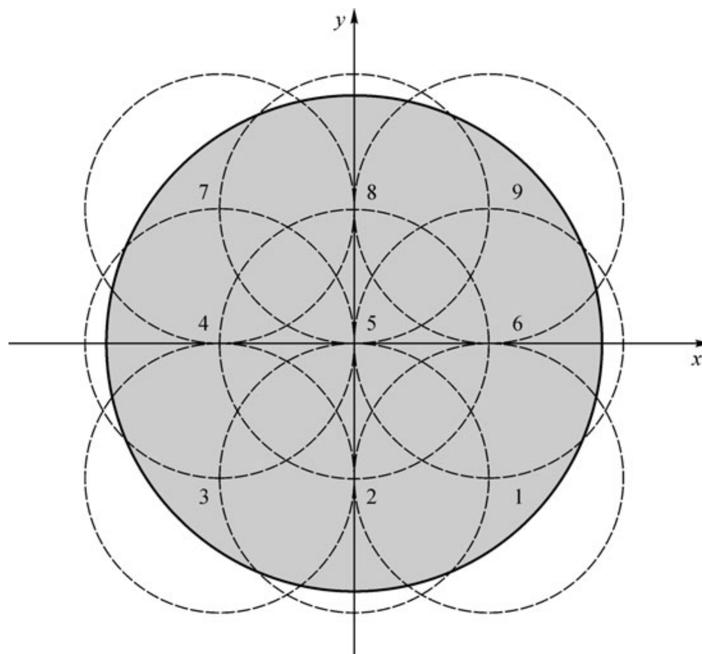

Fig. 5 Dividing method of nine subapertures

Table 2 Stitching precision of nine subapertures ($\lambda = 632.8$ nm)

mode	*PV*	*RMS*	Δ*PV*	Δ*RMS*	single point *RMS*
serial mode	0.920789	0.221889	0.056535	0.005795	0.023636
parallel mode	0.920602	0.227961	0.056348	0.000877	0.004168
partial error averaging mode	0.926446	0.229744	0.062192	0.002059	0.004228
global error averaging mode	0.921775	0.228392	0.057521	0.000708	0.004019

evaluation indexes. The precision of partial error averaging mode is better than that of serial mode. The global error averaging mode and parallel mode have stable and higher precision. From the single point *RMS*, global error averaging mode have the minimum value.

5 Conclusions

This paper presents the basic principle of SAS, and four common stitching modes including serial mode, parallel mode, partial error averaging mode and global error averaging mode were introduced. Then we tested the flat mirror with these four stitching modes using SSI-300. The experiment results of stitching result figures, single point *RMS* figures and stitching precision suggest that the stitching precision of serial mode is the worst. The precision of partial error averaging mode is better than serial mode. The parameters of global error averaging mode and parallel mode are stable and have higher precision. The single point *RMS* of global error averaging mode is the lowest. These results in this paper will be helpful to provide the selection reference for stitching mode in the future.

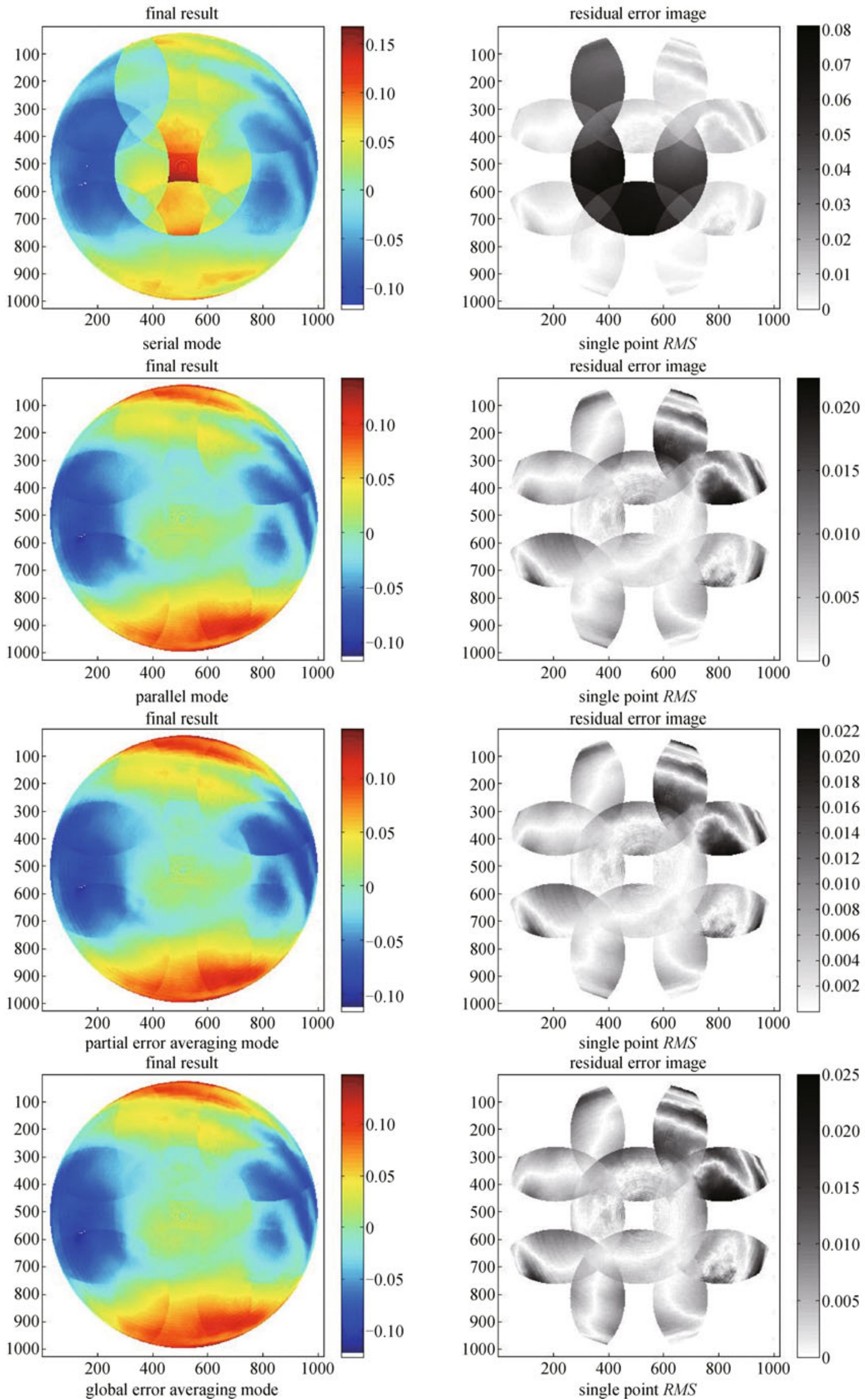

Fig. 6 Stitching results of nine subaperture and single point *RMS* figures in different modes

Acknowledgements This work was supported by the National Natural Science Foundation of China (Grant Nos. 60978043, 61128012, 610611 60503, and 61222506).

References

1. Thetford A. Optical shop testing. Malacara D, ed. John Wiley. Optics & Laser Technology, 1979, 11(1): 55
2. Huxford R B. Wide-FOV head-mounted display using hybrid optics. Proceedings of the International Society for Optics and Photonics, 2004, 5249: 230–237
3. Malacara D. Optical Shop Testing. New York: John Wiley & Sons Inc, 2007
4. Martin H M, Zappellini G B, Cuerden B, Miller S M, Riccardi A, Smith B K. Deformable secondary mirrors for the LBT adaptive optics system. In: Proceedings of the International Society for Optics and Photonics. 2006, 6372
5. Haensel T, Nickel A, Schindler A. Stitching interferometry of aspherical surfaces. In: Proceedings of the International Society for Optics and Photonics. 2001, 4449
6. Shorey A B, Kordonski W, Tricard M. Magnetorheological finishing and subaperture stitching interferometry of large and lightweight optics. In: Proceedings of the International Society for Optics and Photonics. 2004, 5494
7. Murphy P E, Fleig J, Forbes G, Tricard M. High precision metrology of domes and aspheric optics. Proceedings of the International Society for Optics and Photonics, 2005, 5786: 112–121
8. Chen S Y, Li S Y, Dai Y F, Zheng Z W. Testing of large optical surfaces with subaperture stitching. Applied Optics, 2007, 46(17): 3504–3509
9. Thunen J G, Kwon O Y. Full aperture testing with subaperture test optics. Proceedings of the International Society for Optics and Photonics, 1983, 0351: 19–27
10. Chow W W, Lawrence G N. Method for subaperture testing interferogram reduction. Optics Letters, 1983, 8(9): 468–470
11. Stuhlinger T W. Subaperture optical testing: experimental verification. Proceedings of the International Society for Optics and Photonics, 1986, 0655: 350–359
12. Cheng H B, Wang Y W. Research on testing technology for aspheric. Aviation Precision Manufacturing Technology, 2004, 40 (4): 8–10 (in Chinese)
13. Cheng H B, Wang Y W, Feng Z J, Feng Z W, Zhang R. Study on conic constant and paraxial radius of optical aspheric. Optical Technique, 2004, 30(3): 311–313,317 (in Chinese)
14. Gao Y, Tam H Y, Wen Y F, Zhang H J, Cheng H B. Measurement of optical mirror with a small-aperture interferometer. Frontiers of Optoelectronics, 2012, 5(2): 218–223
15. Yun, Y. Research on technique of large aperture optical components test based on sub-aperture stitching. Dissertation for the Master Degree. Changchun: Changchun University of Science and Technology, 2009 (in Chinese)
16. Li X N, Zhang M Y. Study on the sub-aperture stitching interferometry for large plano-optics. Optical Technique, 2006, 32 (4): 514–517 (in Chinese)
17. Chen G, Jiang S L. Large aperture optical components of stitching technique by error averaging. Opto-Electronic Engineering, 2006, 33(6): 118–120 (in Chinese)
18. Otsubo M, Okada K, Tsujiuchi J. Measurement of large plane surface shapes by connecting small-aperture interferograms. Optical Engineering, 1994, 33(2): 608–613
19. Wang C X. Research on the subaperture stitching interferometry for large plano optics. Dissertation for the Master Degree. Nanjing: Nanjing University of Science and Technology, 2007 (in Chinese)
20. Yang J. Research on performance of the subaperture stitching algorithm for optical surfaces. Dissertation for the Master Degree. Changsha: National University of Defense Technology, 2008 (in Chinese)